

## Measurement of the radial diffusion coefficient of galactic cosmic rays near the Earth by the GRAPES-3 experiment

H. Kojima

*Faculty of Engineering, Aichi Institute of Technology, Toyota City, Aichi 470-0392, Japan\**

K. P. Arunbabu, S. R. Dugad, S. K. Gupta,<sup>†</sup> B. Hariharan, P. Jagadeesan, A. Jain,  
P. K. Mohanty, P. S. Rakshe, K. Ramesh, and B. S. Rao

*Tata Institute of Fundamental Research, Mumbai 400 005, India\**

Y. Hayashi and S. Kawakami

*Graduate School of Science, Osaka City University, Osaka 558-8585, Japan\**

T. Nonaka

*Institute for Cosmic Ray Research, Tokyo University, Kashiwa, Chiba 277-8582, Japan\**

A. Oshima and S. Shibata

*College of Engineering, Chubu University, Kasugai, Aichi 487-8501, Japan\**

K. Tanaka

*Graduate School of Information Sciences, Hiroshima City University, Hiroshima 731-3194, Japan\**

M. Tokumaru

*Institute for Space-Earth Environmental Research, Nagoya University, Nagoya, Aichi 446-8601, Japan\**



(Received 16 March 2018; published 9 July 2018)

The flux of galactic cosmic rays (GCRs) is isotropic in the interstellar space. However, in the heliosphere, the ram pressure of outward-moving solar wind convects the GCRs away from the Sun, thereby producing a density gradient in the radial direction. The diffusion of GCRs due to this gradient and scattering with the irregularities in the interplanetary magnetic field (IMF) induce variations in their flux that can be observed near the Earth. A framework for the diffusion-convection mechanism of GCR propagation developed by Parker and collaborators [Phys. Rev. **110**, 1445 (1958); Planet. Space Sci. **13**, 9 (1965); Astrophys. J. **772**, 46 (2013); Space Sci. Rev. **78**, 401 (1996); Astrophys. J. **234**, 746 (1979); Astrophys. J. **361**, 162 (1990); Space Sci. Rev. **176**, 299 (2013)] offers a good description of this phenomenon. One of the outcomes of this framework is an anticorrelation of the variation in solar wind velocity ( $V_{\text{SW}}$ ) and the GCR flux. A second outcome of this gradient in the presence of IMF is the movement of GCRs perpendicular to the ecliptic plane called “Swinson flow.” Therefore, (i) the correlated variations of  $V_{\text{SW}}$  and GCR flux and (ii) the GCR radial density gradient obtained from Swinson flow can each be used to independently measure the radial diffusion coefficient of GCRs in the inner heliosphere. In an earlier work [Phys. Rev. D **91**, 121303(R) (2015)], the GCR flux was shown to be anticorrelated with  $V_{\text{SW}}$  at  $(-1.33 \pm 0.07) \times 10^{-3} \% (\text{km s}^{-1})^{-1}$ . This anticorrelation yields a radial diffusion coefficient  $\kappa = 0.97 \times 10^{19} \text{ m}^2 \text{ s}^{-1}$  at 1 AU. In another work [Astropart. Phys. **62**, 21 (2015)], the measurement of Swinson flow was used to obtain a GCR radial density gradient of  $0.65 \text{ AU}^{-1}$  at a median rigidity of 77 GV. Here, we report a measurement of radial diffusion coefficient  $\kappa = 1.04 \times 10^{19} \text{ m}^2 \text{ s}^{-1}$  at 1 AU from the above-mentioned density gradient, for a mean  $V_{\text{SW}}$  of  $450 \text{ km s}^{-1}$ . Thus, these two distinct approaches essentially yielded similar values of the radial diffusion coefficient  $\kappa = 10^{19} \text{ m}^2 \text{ s}^{-1}$  at 1 AU, characterizing the diffusion of GCRs at 77 GV. From this value of  $\kappa$ , the mean free path length for parallel diffusion  $\lambda_{\parallel}$  was estimated to be 1.2 AU at 77 GV, consistent with earlier reports [Rev. Geophys. Space Phys. **20**, 335 (1982); Astrophys. J. **420**, 294 (1994); Astrophys. J. **604**, 861 (2004)].

DOI: 10.1103/PhysRevD.98.022004

\*GRAPES-3 Experiment, Cosmic Ray Laboratory, Raj Bhavan, Ooty 643 001, India

<sup>†</sup>gupta.crl@gmail.com

## I. INTRODUCTION

High-rigidity ( $\sim 100$  GV) galactic cosmic rays (GCRs) are expected to be isotropic in the interstellar space. The heliosphere is a region of space around the Sun where outward-moving solar wind exerts sufficient ram pressure to resist the GCRs arriving from interstellar space. The heliosphere contains an interplanetary magnetic field (IMF) anchored to the Sun. The IMF is frozen into the solar wind. The anchoring of the IMF to the solar surface combined with the solar rotation forces the IMF into an approximate spiral form. The diffusion of GCRs toward the Sun along the IMF direction and their convection away from the Sun by the solar wind disturbs their isotropy in the heliosphere, unlike in the interstellar region. The convection and diffusion of GCRs from the outer heliosphere to the Sun produce a radial gradient in the density of GCRs [1–5]. This diffusive GCR motion is also influenced by various mechanisms such as the gradient and curvature drifts as well as the movement in the neutral sheet that are especially prominent at lower rigidities [6].

Space weather is a study of the interplanetary medium including the solar wind, the IMF, and the Earth’s magnetosphere. It aims to forecast disruptive processes in the near-Earth environment that are possible. Space weather is important because of the influence it exerts on the reliable operation of technological systems based on both the ground and in space [7]. Large changes in space weather are known to disturb electrical power grids and communication satellites and in extreme cases can endanger the lives of the astronauts [8]. Space weather is largely driven by the solar wind and especially by rapid changes that occur in its velocity  $V_{sw}$ . The modulation of GCRs measured by their intensity variations and/or anisotropy caused by interaction with the IMF offers an effective probe of the dynamics of space weather [9].

The IMF is frozen into the solar wind, resulting in partial trapping of GCRs; therefore, the changes in  $V_{sw}$  are also reflected in the variation of GCR intensity. Thus, a study of the correlation between  $V_{sw}$  and the GCRs offers an excellent probe of space weather. Space weather is influenced by violent phenomena occurring on the surface of the Sun such as the coronal mass ejections (CMEs), solar flares, etc. It also affects the geomagnetic field and the atmosphere through a number of processes. A recent observation by the GRAPES-3 muon telescope showed transient weakening of the Earth’s magnetic field through magnetic reconnection with the southward-directed IMF contained in a CME detected on June 22, 2015 [10]. The study of the strong but rather poorly understood relation between the space weather and its impact on the functioning of various technological systems on the Earth is an important motivation for the deployment of a number of civilian satellites for solar observations by the space agencies from around the world [11].

Generally, the plasma in space displays significant turbulence due to large spatial dimensions involved. The propagation of GCRs in the turbulent magnetic fields present in space plasma plays an important role in providing insights into the astrophysical environments. These effects include solar modulation of the GCRs, their acceleration, transport, anisotropy, etc. However, diffusion of GCRs in a turbulent medium is far from adequately understood [12]. The propagation of GCRs through the heliosphere and especially their interaction with the interplanetary medium in the inner heliosphere impact space weather. The significance of characterizing the GCR propagation is thus self-evident, since it can provide a practical capability of forecasting effects of space weather that has implications for the successful operation of technological infrastructure on the Earth and in space [13].

In brief, the following four processes occur during the transport of GCRs in the heliosphere: (i) outward convection by the solar wind, (ii) inward diffusion due to a density gradient, (iii) particle drifts caused by the gradient and curvature and on a neutral sheet in the turbulent IMF, and (iv) adiabatic cooling. The properties of the interplanetary space near the Earth may be derived from modulation parameters such as the diffusion coefficient, scattering mean free path, etc., that serve as the basic parameters for space weather prediction. The GCR transport equation that describes the above four processes in the heliosphere was first presented by Parker [1] and may be rewritten in a simpler form as

$$\frac{\partial n}{\partial t} + \mathbf{V}_{sw} \cdot \nabla n - \nabla \cdot (\mathbf{K} \cdot \nabla n) - \frac{1}{3} (\nabla \cdot \mathbf{V}_{sw}) \frac{\partial n}{\partial \ln p} = S.$$

Here,  $S$  is the source term,  $\mathbf{K}$  diffusion coefficient tensor, and  $n$  and  $p$  are the GCR density and momentum, respectively. This second-order differential equation can be fully solved by numerical methods. However, full numerical solutions are fairly complex, and therefore approximate solutions of this equation are generally used. This is especially true in modulation studies. Since the overall timescale of variations is long (typically several years) relative to the propagation time through the heliosphere (typically several months), the GCR intensity can be considered to be in quasi-equilibrium. Thus, the source term  $S$  and rate of change of the GCR density  $\frac{\partial n}{\partial t}$  can be ignored. By numerically solving the Fokker-Planck equation, it was shown that effect of the adiabatic cooling becomes very small at rigidities  $> 10$  GV [14]. Thus, the adiabatic term  $\frac{1}{3} (\nabla \cdot \mathbf{V}_{sw}) \frac{\partial n}{\partial \ln p}$  can also be ignored. The lowest-order approximation of the transport equation is the diffusion-convection framework, wherein the GCRs diffuse inward in a spherically symmetric heliosphere as they scatter off the irregularities in the heliospheric magnetic fields, thereby leading to an inward diffusion,  $-\kappa \frac{dn}{dr}$ , here,  $\kappa$  is the “phenomenologically estimated radial diffusion coefficient,” hereafter radial diffusion coefficient,

that is a function of the radial distance  $r$  and GCR rigidity. This inward flux is countered by an outward convective flux  $v n$ , thereby converting the transport equation to its simplest form [5],

$$v n - \kappa \frac{dn}{dr} = 0;$$

here,  $n$  and  $\frac{dn}{dr}$  are the GCR density and its radial density gradient, respectively.  $\kappa$  is the radial diffusion coefficient, and  $v$  is the solar wind velocity.

As discussed above, various phenomena involving anisotropic transport of GCRs in the heliosphere have been investigated within the diffusion-convection framework in the past [1,15]. In this framework, a stationary GCR distribution in the heliosphere results from inward diffusion balancing the outward convection due to solar wind as outlined above. Solar modulation of GCRs up to a median rigidity of 300 GV have been reported in the past [16]. In the present work, data recorded over a duration of six years from the beginning of 2000 to the end of 2005 were carefully analyzed to reduce the contribution of time-dependent solar activity. Therefore, the diffusion-convection equation devoid of any time-dependent term as expressed above was used. Initially, this framework was used to formulate the dynamics of GCR propagation in the heliosphere. However, soon, it was employed to explain the acceleration of particles to high energies in shock waves produced in supernova explosions (Ref. [17] and references therein). Those results clearly indicate that this framework has wider applications and could be used to probe the mechanisms of cosmic ray acceleration in the Galaxy and beyond.

The GCRs, after entering the atmosphere, produce secondaries including mesons that decay into muons. The muons can be studied by detectors located at the ground level. A phenomenon occurring in the interplanetary medium that influences the GCRs would, of course, also affect the muons measured at the ground level. The GCR radial density gradient is a reflection of the mean solar wind velocity  $V_{SW}$ . It is known that  $V_{SW}$  undergoes rapid changes in magnitude. Because of the close link between solar wind and GCRs, the measurement of variation of muon intensity due to changes in  $V_{SW}$  becomes a good tool to probe space weather with muons serving as a proxy of GCRs. The  $V_{SW}$ -GCR correlation has been studied for the past half-century. The earlier correlation studies of the  $V_{SW}$  and GCRs focused on the contribution of active regions or on events such as the solar flares, CMEs, and solar energetic particle events. Early neutron monitor data showed that the streams originating in coronal holes result in reduced flux of GCRs [18]. An anticorrelation between  $V_{SW}$  and GCRs was also recorded in neutron data of 1965–1975 [19]. The data for short-term changes during 1973–1978 displayed a good correlation with the high-speed streams produced in active solar regions [20]. Similar

effects of CMEs on GCR intensity were also shown by several other groups [21]. Such prominent events could have easily produced the observed correlated changes between  $V_{SW}$  and the GCRs. However, in a recent work, this correlation was studied during intervals of low solar activity by removing portions of data that were affected by Forbush decrease (Fd) events, ground-level enhancements (GLEs), and various periodic phenomena [22]. This approach was adopted with a reasonable expectation that the study of space weather during the solar-quiet phase should lead to conclusions that would be complementary to that obtained during the active phase of the Sun. However, during the solar-quiet phase, a much higher sensitivity is required to measure the space weather parameters such as the diffusion coefficient, scattering mean free path, etc. This situation becomes even more challenging if the measurements are performed at high rigidities as in the case of GRAPES-3. The measurement of space weather parameters at high rigidities are important to cover a wide range of energies since high-rigidity GCRs probe a bigger region of interplanetary space due to their longer Larmor radii, thereby facilitating a more comprehensive understanding of space weather. Quantitative measurements of the mean free path in rare scattering free events, in which the mean free path is  $\sim 1$  AU can provide important details of the scattering processes and the magnetic power spectra [23]

The GCR streaming normal to the ecliptic plane causes a sidereal variation due to the inclination of Earth's rotation axis that can be measured by ground-based detectors. The sidereal variation of GCRs below 100 GeV is dominated by Swinson flow. As explained below, this variation results from the streaming of GCRs  $\mathbf{B} \times \mathbf{G}_r$  perpendicular to the ecliptic plane in the north-south direction. Here,  $\mathbf{B}$  represents the IMF, and  $\mathbf{G}_r$  is the fractional radial density gradient of GCRs inside the heliosphere, which is related to  $n$  by the equation  $\mathbf{G}_r = \nabla n/n$  [24]. Since the  $\mathbf{G}_r$  points outward, the flow would reverse its direction with a switch of the IMF polarity. The heliospheric region where the IMF points toward the Sun, named the TW sector, leads to a downward flow. On the other hand, if the IMF points away from the Sun, named the AW sector, which has an upward flow. Thus, the muon telescopes in the northern hemisphere detect their highest rate at 6 h in the AW sectors and 18 h in the TW sectors in local sidereal time. This flow was measured by calculating the difference in amplitudes of variations in the TW and AW sectors by exploiting their asymmetry in the north-south direction [25].

## II. GRAPES-3 EXPERIMENT

The GRAPES-3 experiment is located in Ooty (11.4°N latitude, 76.7°E longitude, and 2200 m altitude) in India. It contains two main detector components, the first a high-density extensive air shower array with a distance of 8 m between two nearest plastic scintillator detectors (each 1 m<sup>2</sup>

area) [26–28]. These scintillator detectors have been deployed on a symmetric hexagonal geometry to provide a relatively uniform coverage. At present, the array is being operated with about 400 scintillator detectors. It was designed to study the GCRs from 10 TeV to 100 PeV and to make precision measurement of their energy spectrum and composition [26,29]. The second detector component is a large area tracking muon telescope, used to measure the muon content of showers produced by GCRs, and provides a high-precision, directional measurement of muon flux. The telescope consists of 16 modules, each module of area of 35 m<sup>2</sup> [30]. The muon telescope is of critical importance for measuring the composition of GCRs [31]. This unique instrument is also used to measure the variation of GCR intensity due to the solar activity [32–35].

The basic detection element of the muon telescope is a proportional counter (PRC) fabricated from a rugged 600 cm long steel pipe of wall thickness of 2.3 mm with a square cross section of 10 × 10 cm<sup>2</sup>. A 35 m<sup>2</sup> module contains 232 PRCs arranged in four layers separated by 15 cm thick concrete. Each layer contains 58 PRCs, with successive layers arranged in mutually perpendicular directions as is seen from Fig. 1. The four-layer configuration of the muon telescope enables the reconstruction of each muon track in two mutually perpendicular planes. Since the vertical separation of two PRC layers in the same projection plane is  $\sim 50$  cm, a muon direction can be measured with an accuracy of  $\sim 4^\circ$ . To achieve an energy threshold of 1 GeV for vertical muons, a total absorber thickness of 550 g cm<sup>-2</sup> in the form of reinforced concrete above the bottom layer of PRCs was used. The concrete overburden was shaped like an inverted pyramid to shield the PRCs with absorber coverage extending up 45° [30]. The muon telescope has a variable energy threshold of  $\sec(\theta)$  GeV for muons incident at a zenith angle  $\theta$ . As shown in Fig. 1, the muon direction is measured for each PRC triggered in the lower layer, and that is then binned into 13 directions based on the location of PRC triggered in

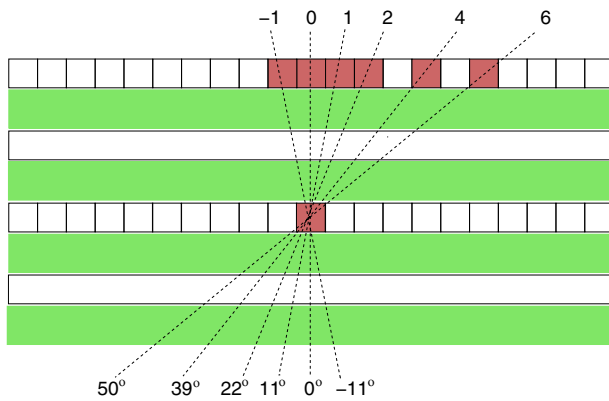


FIG. 1. Muon arrival direction is reconstructed from triggered PRCs, one in the lower layer and one from among 13 PRCs in the upper layer. Triggered PRCs shown as filled squares.

the upper layer from a row of 13 PRCs, one of which is directly above (central PRC), and six each on both sides of the central PRC. This directional binning is carried out in both sets of projection planes, thereby generating a  $13 \times 13 = 169$  solid-angle direction map as shown in Fig. 2. The contents of these 169 directions were recorded at intervals of 10 s, thereby generating a continuous record of directional muon flux. To reduce statistical errors, the 169 directions were combined into nine directions of larger fields of view (FOV) as shown in Fig. 2. This objective was achieved by combining (i) a group of  $3 \times 5$ , or  $5 \times 5$  directions with the exception of the vertical direction, where (ii) the central  $3 \times 3$  directions were combined. This scheme of combination resulted in nearly the same solid-angle coverage for each of the nine directions. It also reduced the dissimilarity in the number of muons recorded in each direction, because of comparatively larger flux of muons for the near central [north (N), east (E), west (W), and south (S)] directions relative to the outer (northeast, southeast, northwest, and southwest) directions. The cutoff rigidity at Ooty was 17 GV in the vertical direction and varied from 14 to 24 GV in the FOV of the telescope. In the present work, the data from (i) only the V direction for the GCR- $V_{SW}$  anticorrelation studies and (ii) only the E and W directions were used for measuring the Swinson flow. A unique feature of the present work was the use of data from different directions for the two independent approaches employed to measure the radial diffusion coefficient  $\kappa$ .

### III. DATA ANALYSIS AND DISCUSSION

The GeV muon detected by GRAPES-3 corresponds to GCR protons of median energy 77 GeV, and that varies from 64 to 92 GeV across the FOV of the telescope. These values of median proton energies were estimated by

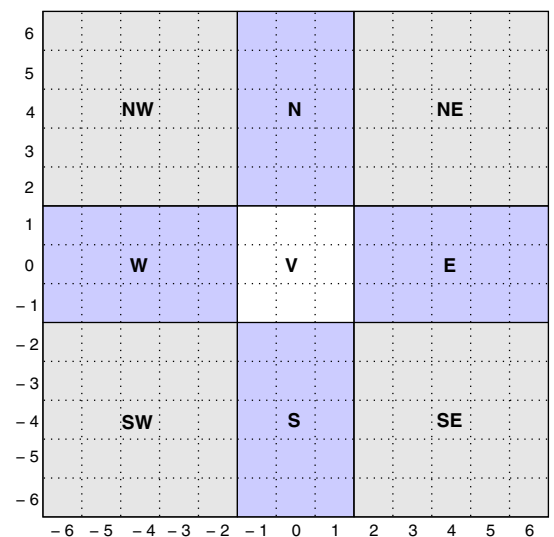


FIG. 2. 169 muon directions combined into nine bigger directions.

using the international geomagnetic reference field model (IGRF-11) of the geomagnetic field [36] and the Monte Carlo simulation CORSIKA code [37]. The GRAPES-3 muon data of six years from January 1, 2000, to December 31, 2005, were used here. In 2000, fewer than 16 modules of the muon telescope were operational, but from January 1, 2001, onward, all 16 modules began operation. During these six years, GRAPES-3 recorded  $\sim 7 \times 10^{12}$  muons that were used to generate a high-precision intensity map of the sky.

After correcting for the dead time, the muon data were separated into intervals of 1 hr for each of the nine directions. A double step cut was used to identify and then remove gaps in data that could distort the actual dependence of GCR intensity on the solar activity. Then, rms deviation  $r_1$  was calculated, and hourly data with deviations in excess of  $10r_1$  were excluded. After calculating the mean, a new rms deviation  $r_2$  was computed, and the data with deviations in excess of  $5r_2$  were excluded in a second cut. This double-cut procedure ensured the removal of sections of low-quality data [22,25]. Thereafter, the muon rates were converted into a percent change with respect to their six year mean after correcting for atmospheric pressure variations [38,39]. The data still contained slow variations caused by the 27 day, the annual, the 11 year, and 22 year solar cycles as well as faster effects such as the sidereal and solar diurnal variations. The long-term periodic variations including the annual, 11 year, and 22 year ones were eliminated by a high-pass filter as explained below. A mean  $Rl_i$  of the hourly muon rate  $r_i$  obtained from 25 hr data centered on that hour served as a low-pass filter. By subtracting mean rate  $Rl_i$  from corresponding observed rate  $r_i$ , high-pass rates  $Rh_i$  were obtained. Only days containing uninterrupted data for 24 hr were included in this analysis [25].

For identifying days affected by aperiodic phenomena such as the Fds, GLEs, etc., data from the Kiel neutron monitor were used, since it showed large amplitude for minor Fds due to a low cutoff rigidity [40]. Detailed criteria used to identify and eliminate the days affected by such activity are explained in earlier work [22,25]. However, to correct for variations in the temperature of the upper atmosphere, as well as other unknown factors, the east-west technique proposed by Kolhörster and others was employed [41–43]. The east-west technique was used to extract the GCR flux along  $V$  by utilizing the data from the E and W along with the time offset  $\tau$  measured between the E and W directions [25]. The days characterized by IMF oriented toward or away from the Sun were identified, during the six year interval. 79% of the data survived this orientation cut. The rest of the data were in a mixed category and were removed. From the daily profiles of AW and TW, the difference  $\frac{(TW-AW)}{2}$  was calculated to obtain a measure of the sidereal anisotropy produced by Swinson flow. The measured profile of the Swinson flow was shown

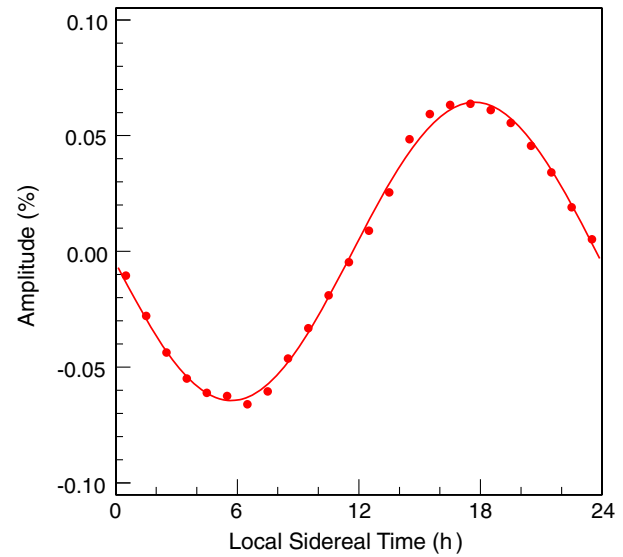


FIG. 3. Sidereal diurnal anisotropy measured by  $\frac{(TW-AW)}{2}$  produced by Swinson flow [25].

in Fig. 7(c) in Ref. [25] and is reproduced here as Fig. 3. The Swinson flow shown in Fig. 3 displays a maximum at  $\sim 18$  h local sidereal time as expected. The amplitude of this tiny variation was  $(0.0644 \pm 0.0008)\%$ . From this amplitude of the Swinson flow, the radial density gradient of GCRs was estimated as  $0.65\% \text{ AU}^{-1}$  at 77 GV [25].

The simplified diffusion-convection equation in its differential form relates the radial density gradient with the velocity of the solar wind by

$$v n - \kappa \frac{dn}{dr} = 0;$$

from above equation, one may obtain the radial density gradient in the neighborhood of the Earth as

$$\frac{1}{n} \frac{dn}{dr} = \frac{v_E}{\kappa},$$

which may be rewritten as

$$\kappa = v_E \times \left( \frac{1}{n} \frac{\Delta n}{\Delta r} \right)^{-1},$$

for solar wind velocity at the Earth  $v_E = 450 \text{ km s}^{-1}$ , and for the radial density gradient of GCRs  $\frac{1}{n} \frac{\Delta n}{\Delta r} = 0.65\% \text{ AU}^{-1}$ , one gets  $\kappa = 1.04 \times 10^{19} \text{ m}^2 \text{ s}^{-1}$ . This value of  $\kappa$  is consistent with the value reported in an earlier work [44].

The diffusion-convection equation in its integral form may be used to relate the variation in  $V_{\text{SW}}$  with corresponding changes in the GCR flux as shown below. Here, the heliosphere is divided into two regions by the radius  $r$ ,  $r = 0$  at the Sun,  $r = r_0 > 1 \text{ AU}$ , and  $r = r_1$  at the

heliospheric boundary. Then, a solution of the simplified diffusion-convection equation in the region  $0 \leq r \leq r_0$  around the Earth may be given by

$$n(r) = n(r_0) \exp\left(-\int_r^{r_0} \frac{v}{\kappa} dr\right),$$

where  $n(r_0)$  is the GCR density deep into heliosphere at  $r = r_0$ . If the region  $0 \leq r \leq r_0$  around the Earth is assumed to be small enough to approximate both  $v$  and  $\kappa$  to be nearly constant, then one obtains

$$n(r) = n(r_0) \exp\left\{\frac{-v(r_0 - r)}{\kappa}\right\},$$

and this when expressed in differential form relative to the velocity  $v$  yields

$$\frac{1}{n} \frac{dn}{dv} = -\frac{(r_0 - r)}{\kappa},$$

which may be rewritten as

$$\kappa = (r - r_0) \left(\frac{\Delta n}{n \Delta v}\right)^{-1};$$

here,  $\frac{\Delta n}{n \Delta v}$  is the fractional change in GCR intensity per unit velocity. This quantity was measured to be  $1.33 \times 10^{-3} \% (\text{km s}^{-1})^{-1}$  [22]. Under quiescent conditions, the changes in the solar wind velocity are not expected to be very rapid. To probe this phenomenon, the correlation between variations in  $V_{\text{SW}}$  with that of GCR flux was studied.

From six years of hourly muon data, the correlation coefficient between  $V_{\text{SW}}$  and GCR flux was calculated as a function of the time shift between them. As expected, an anticorrelation was observed between these two parameters as shown in from Fig. 4. The extreme value of  $-0.36$  of the correlation coefficient is highly significant due to a very large number ( $\sim 50,000$ ) of data points used. The full width at half maximum (FWHM) of the correlation coefficient shown in Fig. 4 is a fairly good measure of the size of the region  $(r_0 - r)$  where the solar wind velocity and the GCR flux remain correlated. The FWHM of the correlation coefficient shown in Fig. 4 is 80 hr, which for a mean  $V_{\text{SW}}$  of  $450 \text{ km s}^{-1}$  yields a size  $((r_0 - r) = 0.864 \text{ AU}$  or  $1.296 \times 10^{11} \text{ m}$ , which may be used to calculate  $\kappa$ ,

$$\kappa = \frac{1.296 \times 10^{11} \text{ m}}{1.33 \times 10^{-8} \text{ m}^{-1} \text{ s}} = 0.97 \times 10^{19} \text{ m}^2 \text{ s}^{-1}.$$

It is interesting to note that the value  $0.97 \times 10^{19} \text{ m}^2 \text{ s}^{-1}$  of radial diffusion coefficient  $\kappa$  measured from the anticorrelation of  $V_{\text{SW}}$  and the GCR flux agrees rather closely with the value of  $1.04 \times 10^{19} \text{ m}^2 \text{ s}^{-1}$  obtained from the density gradient of the GCRs at the same rigidity of

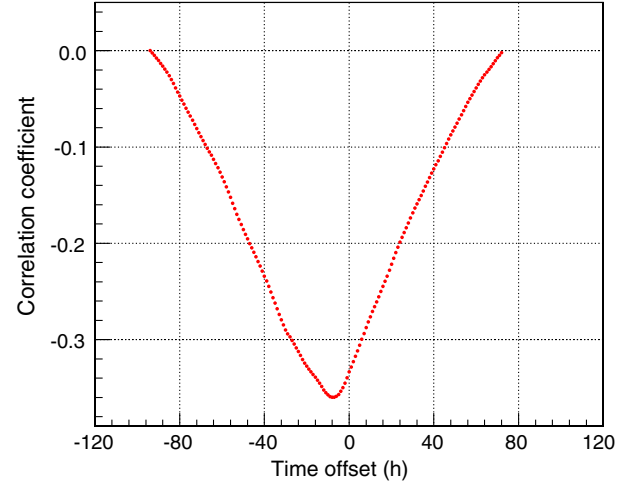


FIG. 4. Correlation coefficient of solar wind velocity and muon flux as a function of their time offset.

77 GV. Although both sets of measurements utilized the GRAPES-3 data for the interval of 2000–2005, the radial density gradient method utilized the data from the E and W directions, while the anticorrelation method used the data from only the V direction. Therefore, not only were the two methods different, but even the two data sets were from distinctly different directions and as such completely independent, which gives greater confidence in the reliability of these conclusions.

The rotation of the Sun distorts the IMF into an Archimedean spiral that creates an angle  $\chi$  between IMF and the radial direction joining the Sun to Earth.  $\chi$  may be calculated as

$$\tan \chi = \frac{2\pi r}{V_{\text{SW}} T},$$

where  $r$  is the radius of Earth's orbit (1 AU),  $V_{\text{SW}}$  is  $450 \text{ km s}^{-1}$ , and  $T$  is the Sun's rotation period (27.3 days),

$$\tan \chi = \frac{2\pi \times 1.5 \times 10^{11}}{4.5 \times 10^5 \times 27.3 \times 86400} = 0.89.$$

The parallel diffusion coefficient  $\kappa_{\parallel}$  may be estimated from the radial diffusion coefficient  $\kappa$  as follows [23]:

$$\kappa_{\parallel} = \frac{\kappa}{\cos^2 \chi} = 1.0 \times 10^{19} \times 1.79 = 1.8 \times 10^{19} \text{ m}^2 \text{ s}^{-1}.$$

Next, by using the relation between the parallel mean free path  $\lambda_{\parallel}$  and the parallel diffusion coefficient  $\kappa_{\parallel}$  [23],

$$\lambda_{\parallel} = \frac{3\kappa_{\parallel}}{c} = 1.8 \times 10^{11} \text{ m} = 1.2 \text{ AU},$$

where  $c$  is the velocity of light as well as that of GCRs.

The parallel mean free path  $\lambda_{\parallel}$  is an important parameter for describing the transport of the GCRs in the interplanetary medium. This topic has been extensively studied over the past several decades. The suitability of the diffusion-convection equation for this study requires the length scale of the processes to be  $l \gg \lambda_{\parallel}$ , as was recently shown by solving the Fokker-Planck equation for isotropic scattering, which is important because the diffusion-convection equation is derived from the Fokker-Planck equation [45]. The applicability of the diffusion-convection framework at low rigidities is well established, and here the high-rigidity GRAPES-3 data are used to study the diffusion of GCRs near the inner heliosphere. It is to be noted that the measured correlation time of 80 hr indicates a correlation length of 1.2 AU, thereby making these measurements sensitive to the region close to the Earth. The use of this correlation and elimination of sporadic solar variability from the data ameliorates concerns regarding the length scale of scattering processes. The close agreement of the measured values of  $\kappa$  by two independent methods indicates that the use of diffusion-convection framework may not be entirely unreasonable. Since an understanding of the propagation process of the GCRs is the key to the emerging field of cosmic ray astronomy, it is hoped that these results may motivate a debate on the applicability of the diffusion-convection framework for the propagation of high-rigidity GCRs. This work also highlights the need for an appropriate theoretical framework suited for interpreting the high-rigidity data collected by the AMS-02 Collaboration [46].

Detailed simulations estimating  $\lambda_{\parallel}$  as a function of rigidity predict a rapid rise in the value of  $\lambda_{\parallel}$  at high rigidities ( $> 10$  GV) [23]. The GRAPES-3 value of  $\lambda_{\parallel} = 1.2$  AU at 77 GV agrees rather closely with the predicted value of  $\sim 1$  AU based on simulations at the same rigidity [47]. The calculations of  $\lambda_{\parallel}$  in partially turbulent electromagnetic fields in the damping model of dynamical turbulence for pure two-dimensional turbulent geometry were carried out for the pitch-angle Fokker-Planck coefficient for pure slab geometry. At a rigidity of 77 GV, the value of  $\lambda_{\parallel}$  agrees with the value obtained from GRAPES-3 [48]. Another group has developed a hybrid plasma-wave/magnetostatic turbulence model, and using a test particle code to describe the scattering of GCRs and their calculated value of  $\lambda_{\parallel}$  shows good agreement with the GRAPES-3 result [49].

#### IV. CONCLUSION

The space weather studies through the diffusion of high-energy GCRs are extremely valuable since they serve as a probe of relatively larger scale structures in the interplanetary space and provide information complementary to that obtained from the low-energy measurements using space-based probes and neutron monitors. The analysis of GRAPES-3 muon data of six years yielded a radial diffusion coefficient  $\kappa = 0.97 \times 10^{19} \text{ m}^2 \text{ s}^{-1}$  at 1 AU from GCR intensity and solar wind velocity correlation. A similar value of  $\kappa = 1.04 \times 10^{19} \text{ m}^2 \text{ s}^{-1}$  at 1 AU was obtained from the radial density gradient of GCRs by Swinson flow. Thus, two independent methods yielded similar values  $\kappa = 10^{19} \text{ m}^2 \text{ s}^{-1}$  at 1 AU at a median GCR rigidity of 77 GV. This value of  $\kappa$  and a mean free path length of 1.2 AU was estimated for parallel diffusion  $\lambda_{\parallel}$  in close agreement with the theoretical values obtained from simulations. In the present study, data from the solar-quiet phase was used to eliminate large variability caused by high solar activity to measure the underlying parameters of space weather physics such as the radial diffusion coefficient and the mean free path length for parallel diffusion. This information may even turn out to be helpful in arriving at a more rigorous understanding of the space weather phenomenon during high solar activity.

#### ACKNOWLEDGMENTS

We thank D. B. Arjunan, S. Kingston, K. Manjunath, S. Murugapandian, B. Rajesh, V. Santhosh Kumar, M. S. Shareef, C. Shobana, and R. Sureshkumar for help in the operation, maintenance of the proportional counters, and associated electronics for the GRAPES-3 muon telescope. We thank G. P. Francis, V. Jeyakumar, and K. Ramadass for help in the repair and maintenance of various mechanical components of the muon telescope. Easy availability of the OMNI data from the GSFC/SPDF OMNIWeb interface at [50] made it possible to determine the IMF direction, a critical requirement for the analysis of data. Use of the Kiel neutron monitor data was very useful, for which we are grateful to the Kiel group. We thank T. Terasawa for important discussions. This work was partially supported by the grants of the ISEE of Nagoya University; Chubu University; and the Ministry of Education, and Science, Japan. We thank the anonymous referee whose incisive comments significantly improved the flow of the arguments presented here.

- [1] E. N. Parker, *Phys. Rev.* **110**, 1445 (1958); *Planet. Space Sci.* **13**, 9 (1965); N. E. Engelbrecht and R. A. Burger, *Astrophys. J.* **772**, 46 (2013).
- [2] D. L. Hall, M. L. Duldig, and J. E. Humble, *Space Sci. Rev.* **78**, 401 (1996).
- [3] P. A. Isenberg and J. R. Jokipii, *Astrophys. J.* **234**, 746 (1979).
- [4] F. C. Jones, *Astrophys. J.* **361**, 162 (1990).
- [5] H. Moraal, *Space Sci. Rev.* **176**, 299 (2013).
- [6] F. F. Chen, *Introduction to Plasma Physics and Controlled Fusion*, 3rd ed. (Springer, Berlin, 2016).
- [7] K. Kudela *et al.*, *Space Sci. Rev.* **93**, 153 (2000).
- [8] D. N. Baker, *Adv. Space Res.* **22**, 7 (1998).
- [9] M. L. Goldstein, D. A. Roberts, and W. H. Matthaeus, *Annu. Rev. Astron. Astrophys.* **33**, 283 (1995).
- [10] P. K. Mohanty, K. P. Arunbabu, T. Aziz, S. R. Dugad, S. K. Gupta, B. Hariharan, P. Jagadeesan, A. Jain, S. D. Morris, B. S. Rao, Y. Hayashi, S. Kawakami, A. Oshima, S. Shibata, S. Raha, P. Subramanian, and H. Kojima, *Phys. Rev. Lett.* **117**, 171101 (2016).
- [11] <http://science.gsfc.nasa.gov/sed/index.cfm>.
- [12] S. Xu and H. Yan, *Astrophys. J.* **779**, 140 (2013).
- [13] R. Modzelewska, in *Proceedings of the 33rd ICRC, Rio de Janeiro, Brazil, 2013*, 1176 (unpublished).
- [14] Y. Yamada, S. Yanagita, and T. Yoshida, *Geophys. Res. Lett.* **25**, 2353 (1998).
- [15] A. Shalchi, *Nonlinear Cosmic Ray Diffusion Theories*, *Astrophysics and Space Science Library* (Springer, Berlin, 2009), Vol. 362.
- [16] K. Munakata, M. Kozai, C. Kato, and J. Kóta, *Astrophys. J.* **791**, 22 (2014).
- [17] W. I. Axford, *Astrophys. J. Suppl. Ser.* **90**, 937 (1994).
- [18] N. Iucci, M. Parisi, M. Storini, and G. Villorosi, *Nuovo Cimento* **2**, 421 (1979).
- [19] Y. Munakata and K. Nagashima, in *Proceedings of the 16th ICRC, Kyoto, Japan, 1979* (ICRR, University of Tokyo, 1979), vol. 3, p. 530.
- [20] D. Venkatesan, A. K. Shukla, and S. P. Agrawal, *Sol. Phys.* **81**, 375 (1982).
- [21] E. W. Cliver, A. G. Ling, and I. G. Richardson, *Astrophys. J.* **592**, 574 (2003); A. Lara, N. Gopalswamy, R. A. Caballero-Lopez, S. Yashiro, H. Xie, and J. F. Valdes-Galicia, *Astrophys. J.* **625**, 441 (2005).
- [22] H. Kojima, H. M. Antia, S. R. Dugad, S. K. Gupta, P. Jagadeesan, A. Jain, P. K. Mohanty, B. S. Rao, Y. Hayashi, S. Kawakami, T. Nonaka, A. Oshima, S. Shibata, and K. Tanaka, *Phys. Rev. D* **91**, 121303(R) (2015).
- [23] I. D. Palmer, *Rev. Geophys. Space Phys.* **20**, 335 (1982).
- [24] D. B. Swinson, *J. Geophys. Res.* **74**, 5591 (1969); **81**, 2075 (1976).
- [25] H. Kojima *et al.*, *Astropart. Phys.* **62**, 21 (2015).
- [26] S. K. Gupta *et al.*, *Nucl. Instrum. Methods Phys. Res., Sect. A* **540**, 311 (2005).
- [27] P. Mohanty, S. Dugad, U. Goswami, S. Gupta, Y. Hayashi, A. Iyer, N. Ito, P. Jagadeesan, A. Jain, and S. Karthikeyan, *Astropart. Phys.* **31**, 24 (2009).
- [28] P. K. Mohanty, S. R. Dugad, and S. K. Gupta, *Rev. Sci. Instrum.* **83**, 043301 (2012).
- [29] S. K. Gupta *et al.*, *Nucl. Phys. B, Proc. Suppl.* **196**, 153 (2009).
- [30] Y. Hayashi *et al.*, *Nucl. Instrum. Methods Phys. Res., Sect. A* **545**, 643 (2005).
- [31] H. Tanaka *et al.*, *J. Phys. G* **39**, 025201 (2012).
- [32] T. Nonaka, Y. Hayashi, N. Ito, S. Kawakami, T. Matsuyama, A. Oshima, H. Tanaka, T. Yoshikoshi, S. K. Gupta, A. Jain, S. Karthikeyan, P. K. Mohanty, S. D. Morris, B. S. Rao, K. C. Ravindran, K. Sivaprasad, B. V. Sreekantan, S. C. Tonwar, K. Viswanathan, and H. Kojima, *Phys. Rev. D* **74**, 052003 (2006).
- [33] P. Subramanian *et al.*, *Astron. Astrophys.* **494**, 1107 (2009).
- [34] K. P. Arunbabu, H. M. Antia, S. R. Dugad, S. K. Gupta, Y. Hayashi, S. Kawakami, P. K. Mohanty, T. Nonaka, A. Oshima, and P. Subramanian, *Astron. Astrophys.* **555**, A139 (2013).
- [35] K. P. Arunbabu, H. M. Antia, S. R. Dugad, S. K. Gupta, Y. Hayashi, S. Kawakami, P. K. Mohanty, A. Oshima, and P. Subramanian, *Astron. Astrophys.* **580**, A41 (2015).
- [36] C. C. Finlay *et al.*, *Geophys. J. Int.* **183**, 1216 (2010).
- [37] <http://www-ik.fzk.de/corsika>.
- [38] P. K. Mohanty *et al.*, *Pramana J. Phys.* **81**, 343 (2013).
- [39] P. K. Mohanty *et al.*, *Astropart. Phys.* **79**, 23 (2016).
- [40] <http://134.245.132.179/kiel/main.htm>.
- [41] W. Kolhörster, *Phys. Z.* **42**, 55 (1941).
- [42] H. Alfvén and K. G. Malmfors, *Ark. Mat. Astron. Fys.* **29A**, 24 (1943).
- [43] H. Elliot and D. W. N. Dolbear, *J. Atmos. Terr. Phys.* **1**, 205 (1951).
- [44] S. Yasue, *J. Geomagn. Geoelectr.* **32**, 617 (1980).
- [45] M. A. Malkov, *Phys. Rev. D* **95**, 023007 (2017).
- [46] M. Aguilar *et al.*, *Phys. Rev. Lett.* **114**, 171103 (2015).
- [47] J. W. Bieber, W. H. Matthaeus, C. W. Smith, W. Wanner, M.-B. Kallenrode, and G. Wibberenz, *Astrophys. J.* **420**, 294 (1994).
- [48] A. Shalchi, and R. Schlickeiser, *Astrophys. J.* **604**, 861 (2004).
- [49] R. C. Tautz and A. Shalchi, *J. Geophys. Res. Space Phys.* **118**, 642 (2013).
- [50] <http://omniweb.gsfc.nasa.gov>.